JOURNAL OF CATALYSIS **101**, 81–89 (1986)

^{31}P-MASNMR Spectroscopic Studies with Zirconium Phosphate Catalysts

KOH-ICHI SEGAWA[1] AND YASUO NAKAJIMA

Department of Chemistry, Faculty of Science and Technology, Sophia University, 7-1 Kioi-cho Chiyoda-ku, Tokyo 102, Japan

AND

SHIN-ICHI NAKATA, SACHIO ASAOKA, AND HIROMITSU TAKAHASHI

R & D Center, Chiyoda Chemical Engineering & Construction Co., Ltd., 3-13 Moriya-cho Kanagawa-ku, Yokohama 221, Japan

Received October 29, 1985; revised April 18, 1986

Zirconium phosphates are crystallized during the removal of hydration water in the zirconium phosphate gel with phosphoric acid solution under reduced pressure. Several forms of crystallites are obtained by this procedure, depending on the temperature and process time, for a given concentration of phosphoric acid. Synthetic ZrP_2O_7 and ε-$Zr(HPO_4)_2$ catalysts, which were evacuated at 773 K, showed higher catalytic activities for butene isomerization than other forms of zirconium phosphates or other conventional solid acid catalysts. In order to elucidate those higher catalytic activities, ^{31}P magic angle spinning NMR (^{31}P-MASNMR) has been employed to study zirconium phosphates after evacuation at different temperatures. The ^{31}P chemical shifts move towards higher magnetic fields as the layer separations become smaller. The catalysts which showed higher activities showed higher chemical shifts at around −38 ppm from H_3PO_4. These results suggest that the phosphate groups remaining after evacuation at around 800 K may enhance the protonic characteristics, since the accumulation of electrons moves from the phosphate groups on the surface to phosphorus atoms which are located between Zr atom planes.

INTRODUCTION

Acid salts of tetravalent metals, whose compounds have the general formula $M(HXO_4)_2 \cdot nH_2O$ (M: tetravalent metal; X: P, As), can be obtained in amorphous forms or in various crystalline forms having layered or three-dimensional structures (*1*).

A metal hydrogen phosphate catalyst generally has acid-catalyzed properties. Most metal phosphate catalysts are hydrated forms of amorphous gels or acid salts. For these materials, it is rather hard to discriminate the active sites of catalysts, because heat treatments have complicated their structures.

The previous papers (*2, 3*) showed that ε-$Zr(HPO_4)_2$ (abbreviated as ε-ZrP) catalyst, which was evacuated at high temperatures (ca. 800 K), exhibited higher catalytic activities for 1-butene isomerization than other forms of zirconium phosphates, such as α-$Zr(HPO_4)_2 \cdot H_2O$ (abbreviated as α-ZrP), zirconium phosphate gel (abbreviated as ZrP-gel), or other conventional solid acid catalysts. For ε-ZrP after evacuation at 773 K, most phosphate groups were removed, with consequent loss of water, due to the condensation of phosphate groups between each zirconium atom layer. However, a trace amount of residual phosphate groups still remained on the surface. The co-isomerization reaction of d_0- and d_8-1-butene suggests that isomerization would proceed on protonic acid sites even after heat treatment at 773 K (*2*). Even though the pro-

---

[1] To whom all correspondence should be addressed.

0021-9517/86 $3.00

tonic concentrations decreased, the reaction rates for isomerization were drastically enhanced. It is very important to know the reason for the enhancement of protonic character on zirconium phosphate (abbreviated as ZrP) catalysts after evacuation at such high temperatures (ca. 800 K). This work elucidates the higher catalytic activities for ZrP. We studied the phosphorus microenvironment for ZrP after calcination at various temperatures by high-resolution solid state ^{31}P magic angle spinning NMR (^{31}P-MASNMR), and we compared the *cis*-2-butene isomerization activities for some specific surfaces. ^{31}P-MASNMR spectra of various crystal phases of ZrP must be distinguished by either their isotropic chemical shifts or their ^{31}P chemical shift anisotropies.

EXPERIMENTAL

Preparation of ZrP. Addition of a soluble Zr(IV) salt ($ZrO(NO_3)_2 \cdot 2H_2O$; 0.4 mol · dm^{-3}) to phosphoric acid (1 mol · dm^{-3}) results in the precipitation of a gelatinous amorphous solid. This ZrP-gel was washed with distilled water; filtration and drying at 330 K for 50 h followed. The resulting ZrP-gel has 7.8 mol of water of crystallization (part of which is hydrated water) per Zr atom.

The stoichiometric crystalline zirconium phosphate can be prepared by refluxing ZrP-gel in concentrated phosphoric acid (*4*). But we found α-ZrP and ε-ZrP were very well crystallized during the removal of water of crystallization by heating with phosphoric acid solution under reduced pressure. By this procedure, highly crystalline zirconium phosphates have been obtained in a shorter process time. For α-ZrP, ZrP-gel (100 g) was mixed with phosphoric acid solution (15 mol · dm^{-3}, 300 ml); then the mixture was heated to 408 K from room temperature at a constant temperature increase in 90 min, and held at this temperature for 3 h. For ε-ZrP, a slurry of ZrP-gel with phosphoric acid solution (same as α-ZrP) was heated to 453 K from room temperature at a constant temperature increase in 3 h, and was then kept at 453 K for another 3 h. In both cases, the preparation system operated under reduced pressure at 2.7 kPa; the water which evolved during the heat treatment was removed from the sidearm attached to the preparation system. Synthetic zirconium diphosphate (abbreviated as pyro-ZrP(syn)) was prepared by the same procedure. The slurry of ZrP-gel with phosphoric acid solution was heated to 673 K under reduced pressure (2.7 kPa) in 3 h. X-Ray diffraction (XRD) patterns of pyro-ZrP(syn) showed exactly the same patterns of cubic zirconium diphosphate (abbreviated as pyro-ZrP) (*5*) as those which had been obtained by calcination of ZrP-gel above 1323 K. All the resulting crystals were washed and dried at room temperature under vacuum conditions.

Catalytic reactions. Isomerization of *cis*-2-butene (12 kPa) was carried out at 313 K by using a closed recirculation system. Prior to reaction, the catalyst was evacuated at a specified temperature. The reaction products were analyzed by a gas chromatograph which was equipped with a 6-m column of VZ-7 at 288 K.

XRD and thermal analysis. The procedures for measurements have been described in detail elsewhere (*2*).

^{31}P-MASNMR spectroscopy. ^{31}P-MASNMR has been employed for ZrP after evacuation at different temperatures. The ^{31}P-MASNMR spectra were obtained at 109.38 MHz on a Fourier transform pulsed NMR spectrometer (JEOL JNM-GX270) which was equipped with a CP/MAS unit (JEOL NM-GSH27MU). Samples for NMR weighed ca. 0.3 g; they were prepared in a dry-nitrogen atmosphere, then packed firmly in Delin rotors with press-fit Teflon caps. Spinning speeds, ν_{rot}, determined from the side band spacing in spinning spectra, were 3.6 to 4.0 kHz. All ^{31}P-NMR spectra combined with magic angle spinning (MAS) spectra were measured with proton decoupling during data acquisition. Cross polarization (CP) was not employed,

TABLE 1

Catalytic Activities and Selectivities for Isomerization of *cis*-2-butene on Various Solid Acid Catalysts

Catalyst	Evacuation temp. (K)	Reaction rate[a] (10^{10}/mol · s^{-1} · m^{-2})	*trans*/1[b]	Surface area (m^2 · g^{-1})
ZrP-gel	313	0	—	5.4
	773	107	2.6	4.9
	1323	0	—	2.0
α-ZrP	313	0	—	11.6
	773	27	2.5	12.3
	973	200	4.0	12.5
	1323	0	—	2.1
ε-ZrP	453	3	1.5	4.5
	773	880	4.0	5.0
	1473	0	—	2.3
Pyro-ZrP(syn)	473	106	2.5	2.8
	773	6071	3.0	2.8
	1323	0	—	2.5
Al_2O_3[c]	773	30	12.0	177.0
SiO_2–Al_2O_3[d]	773	270	2.0	560.0

[a] Initial rate of isomerization: reaction temp. = 313 K; P_{cis} = 12 kPa.
[b] Initial product ratio: *trans*-2-butene/1-butene.
[c] JRC (Japan Reference Catalyst)-ALO-4.
[d] JRC (Japan Reference Catalyst)-SAL-2.

since the protons do not attach directly to ^{31}P nuclei; 8K data points were collected with 20 to 30 scans accumulated per spectrum at a delay of 14 s between 90° pulses. ^{31}P chemical shifts were determined by replacing the sample rotor with a rotor containing phosphoric acid (15 mol · dm^{-3}), and observing its resonance frequency in the absence of spinning.

RESULTS AND DISCUSSION

Catalytic Reactions

The catalytic isomerization of *cis*-2-butene over various forms of ZrP were measured. The results are summarized in Table 1. If we compare them with the previous results (*2*), we see that the ε-ZrP catalysts which were evacuated at 773 K showed higher catalytic activities (based on unit surface area) than α-ZrP and ZrP-gel or other conventional solid acid catalysts, such as Al_2O_3 (JRC-ALO-4) and SiO_2-Al_2O_3 (JRC-SAL-2). The pyro-ZrP(syn) catalyst had the highest activity. For all ZrP catalysts in Table 1, the activities show enhancements of reaction rates after evacuation at higher temperatures (773–973 K).

The ring opening isomerization of cyclopropane and co-isomerization of d_0- and d_8-1-butene suggested that isomerization would have proceeded on protonic acid sites even after heat treatment at 773 K (*2*). On the other hand, the ZrP catalysts, which were evacuated above ca. 1300 K, showed no catalytic activities for isomerization. In those temperature regions for calcination, the crystals were changed to pyro-ZrP(cubic) (*5*), as confirmed by XRD measurements.

Thermal Analysis

The temperature-programmed decomposition(TPDE) spectra under vacuum conditions of ZrP-gel, α-ZrP, ε-ZrP, and pyro-ZrP(syn) are shown in Fig. 1. The TPDE spectrum of ZrP-gel (A in Fig. 1) showed a

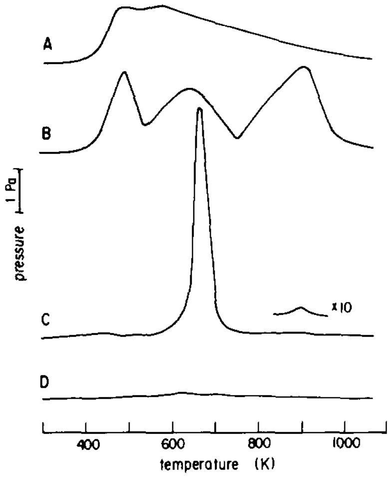

FIG. 1. TPDE spectra of zirconium phosphates: (A) $Zr(HPO_4)_2 \cdot nH_2O$ (ZrP-gel), (B) α-$Zr(HPO_4)_2 \cdot H_2O$ (α-ZrP), (C) ε-$Zr(HPO_4)_2$ (ε-ZrP), (D) synthetic ZrP_2O_7 (pyro-ZrP(syn)).

broad peak which suggests that elimination of water of crystallization and condensation of phosphate groups (2) have occurred in similar temperature regions. Prior to the TPDE experiment, ZrP-gel was evacuated at room temperature (up to 1×10^{-4} Pa). During this treatment, most of the hydrated water molecules were removed; thus, about one-half mole of water molecules has been removed in the TPDE experiment. Therefore, the final chemical composition of ZrP-gel was $Zr(HPO_4)_2 \cdot 0.5H_2O$. The TPDE spectrum of α-ZrP (B in Fig. 1) showed three-stage dehydration. This result was different from our previous result (*2*), which showed two-stage dehydration. This is because of the different crystallinity of α-ZrP, due to the different preparation procedures. Even though the XRD patterns were the same in both α-ZrP samples, the reflection intensities of the present sample were much stronger than those of the previous one. Clearfield and Pack (*6*) reported several thermal analysis results for several α-ZrP crystals obtained by different phosphoric acid concentrations in the refluxing process. They conclude that the thermal behavior difference is connected with crystal perfection, as manifested by the changes in unit cell dimensions which occur on refluxing. In the case of α-ZrP (B in Fig. 1), the elimination of 1 mol of water of crystallization in two stages is shown by the two lower temperature peaks (two kinds of water of crystallization in different environments). The third stage is due to the condensation of phosphate groups (*2*). For ε-ZrP (C in Fig. 1), the spectrum showed one-stage dehydration due to the condensation of phosphate groups with consequent loss of 1 mol of water, since ε-ZrP is a nonhydrated form. However, a trace amount of water evolved in the higher temperature region (ca. 900 K). These residual phosphate groups would be the surface protonic sites on the corners and edges of crystals (*2, 3*). Finally, the TPDE spectrum of pyro-ZrP (syn) has been measured (D in Fig. 1). A very small amount of water (1–2%) was evolved during the TPDE run, which suggests that the pyro-ZrP(syn) also has phosphate groups, even if the XRD patterns were the same as those for cubic zirconium diphosphate (pyro-ZrP).

XRD Measurements

XRD patterns of ZrP evacuated at different temperatures are shown in Figs. 2 to 4. The XRD patterns of ZrP-gel do not show any crystal phases after evacuation below

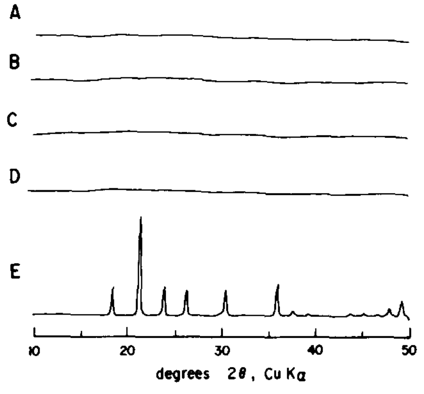

FIG. 2. XRD patterns of ZrP-gel evacuated at different temperatures: (A) room temp., (B) 473 K, (C) 773 K, (D) 1073 K, (E) 1323 K.

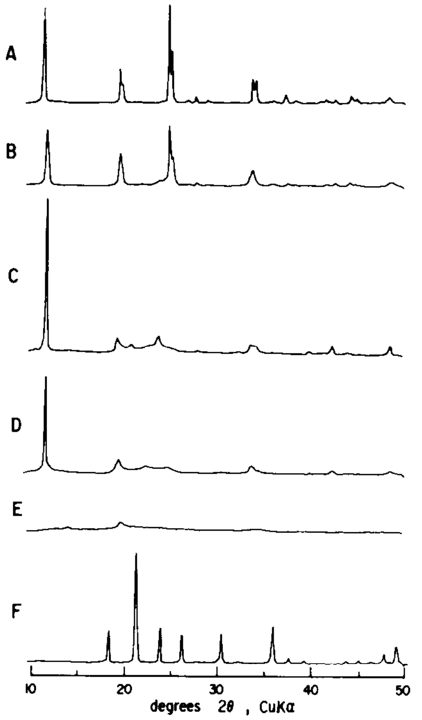

FIG. 3. XRD patterns of α-ZrP evacuated at different temperatures: (A) room temp., (B) 523 K, (C) 773 K, (D) 848 K, (E) 1073 K, (F) 1323 K.

1073 K (A to D in Fig. 2). When the ZrP-gel was heated at 1323 K, the crystals changed to pyro-ZrP. In spite of the rather broadened reflection of XRD, ZrP-gel has been considered to be a layered compound (*4*), whose general formula is $Zr(HPO_4)_2 \cdot nH_2O$). ZrP-gel also shows ionic exchange capabilities (*7*).

The most extensively investigated ZrP is the α-layered acid salt, which is usually obtained as the monohydrated form (*8*). α-ZrP crystallizes in the monoclinic system (*9*). The Zr atoms lie very nearly in a plane and are bridged by phosphorous tetrahedra (phosphate group). These are situated alternately above and below the Zr atom plane. Three oxygen atoms of each phosphate group are bonded to three different Zr atoms, which form a distorted equilateral triangle. Thus, each Zr atom is octahedrally coordinated by oxygens. The proton of the phosphate group is attached to the fourth oxygen, which is directed toward the interlayer space above and below Zr atom planes. The layer separation of α-ZrP is about 0.76 nm, which is about 0.2 nm larger than ε-ZrP (2). Between each layer there are cavities which are filled with water of crystallization, and these are stabilized by hydrogen bonding between phosphate groups (*10*). After removal of water of crystallization, the lattice eventually became increasingly disordered with increasing temperature (773–1073 K), finally changing to pyro-ZrP above 1323 K; these effects are shown in Fig. 3. Figure 4 shows that the layer separation of Zr atom planes for ε-ZrP is about 0.56 nm (*2*). When the crystals were evacuated at higher temperatures (700–1100 K), the XRD peaks quickly changed to patterns similar to those of pyro-ZrP.

Finally, regardless of the original structure of ZrP, when the ZrP was heated at

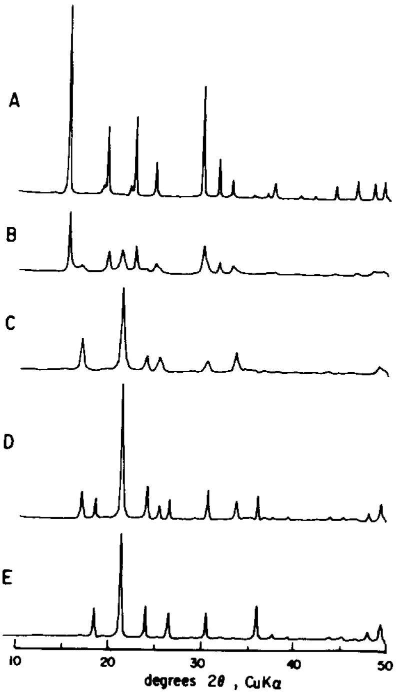

FIG. 4. XRD patterns of ε-ZrP evacuated at different temperatures: (A) room temp., (B) 573 K, (C) 773 K, (D) 873 K, (E) 1473 K.

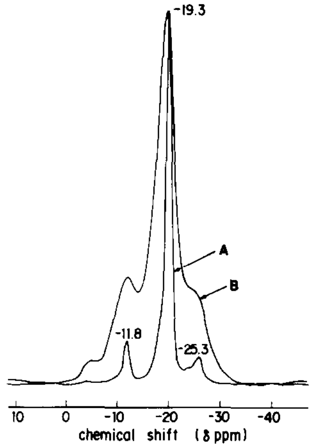

FIG. 5. ^{31}P-MASNMR spectra of ZrP-gel: (A) hydrated form, (B) evacuated at room temperature.

1323–1473 K (see Figs. 2 to 4), crystals changed to complete pyro-ZrP, which has no phosphate groups in the crystals.

^{31}P-MASNMR Spectroscopy

During the heat treatments of ZrP, phosphate groups were converted to P–O–P bondings (*2*), due to the condensation of phosphate groups between each layer. Therefore, phosphorus environments of ZrP during and after condensation of phosphate groups must be different from either original structure. The structural changes in ZrP caused by heat treatments are hard to distinguish by XRD experiments, since serious broadened reflections are observed at higher evacuation temperatures (see Figs. 2 and 3).

The ^{31}P-MASNMR spectrum of ZrP-gel (A in Fig. 5) showed three different sharp peaks at −11.8 ppm, −19.7 ppm (major), and −25.5 ppm from H_3PO_4. This result suggests that ZrP-gel has three kinds of phosphorus environments, which correspond to the different environments of phosphate groups. When ZrP-gel was evacuated at room temperature, the peaks broadened (B in Fig. 5). The broad linewidths of these signals changed into much narrower ones without changing the chemical shifts when the hydration for dehydrated sample ($Zr(HPO_4)_2 \cdot 0.5H_2O$) took place, in agreement with the increase of a mobility for phosphorus surroundings. When ZrP-gel was evacuated at higher temperatures (473–1073 K) in Fig. 6, the chemical shifts gradually shifted toward higher magnetic fields at −29.5 ppm. This sample was changed to amorphous zirconium diphosphate (see Figs. 1A and 2D); then the crystals changed to pyro-ZrP at 1323 K (E in Fig. 6), which consisted of five different peaks from −32 to −43 ppm. Corbridge suggested the presence of five different kinds of configurations in condensed phosphates (pyro-ZrP) (*11*), which correspond to either the *cis* or *trans* form of linear and bent P–O–P bonds. Those different phosphorus environments would affect the spectrum. For α-ZrP (Fig. 7) and ε-ZrP (Fig. 8), only one ^{31}P resonance was observed, at −16.6 or −21.7 ppm. The order of the chemical shift of the resonance of α-ZrP, ZrP-gel, and ε-ZrP corresponds to decreasing amounts of water of crystallization. For α-ZrP in Fig. 7, the crystals which were evacuated at room temperature, 523 K (after first stage in Fig. 1B), and 773 K (after second stage in Fig. 1B) showed three identical resonance lines at −16.6, −17.5, and −19.5 ppm, with very narrow linewidths, indicating small chemical shift anisotropies. In the temperature region below 773 K, the phase transitions from α-ZrP via ζ-ZrP to η-ZrP have been observed (*12*). The three different crystal phases have different layer separations of Zr atom planes (α: 0.76 nm, ζ: 0.74 nm, η: 0.72 nm) (*6*). During the removal of water of crystallization, phase changes in α-ZrP may occur at different treatment temperatures; these phase changes occur in temperature regions similar to those of the first and second stages of the TPDE spectrum in Fig. 1B. α-ZrP evacuated at 1073 K showed one broader resonance peak at −31 ppm (E in Fig. 7); this is similar to spectrum D in Fig. 6. Our XRD results and thermal analysis for this stage show that crystals changed to amorphous zirconium diphosphate. Fi-

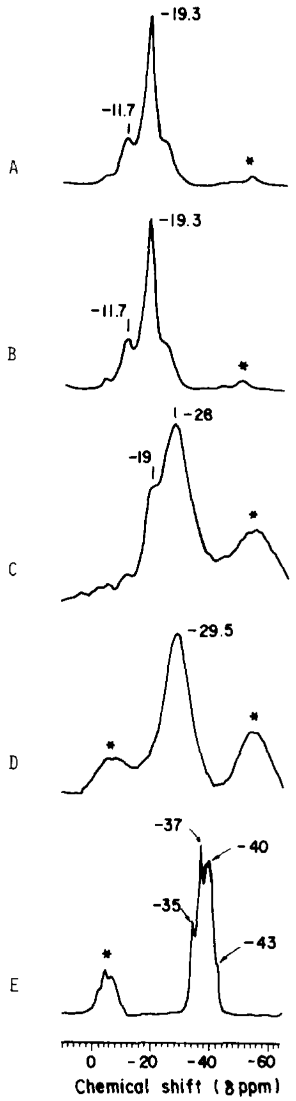

FIG. 6. ^{31}P-MASNMR spectra of ZrP-gel evacuated at different temperatures: (A) room temp., (B) 473 K, (C) 773 K, (D) 1073 K, (E) 1323 K. * Spinning side band (SSB).

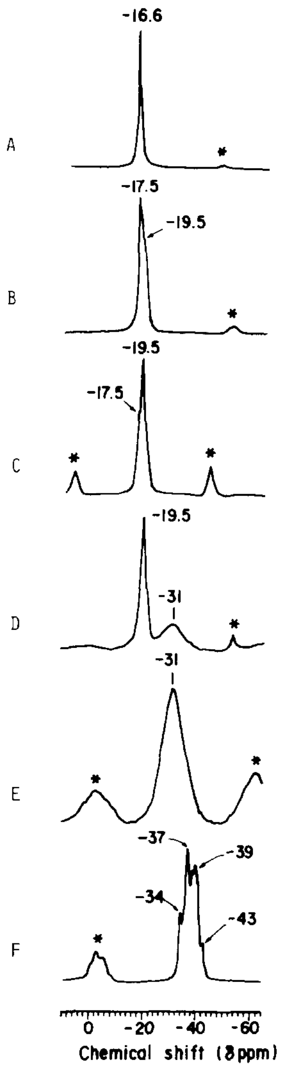

FIG. 7. ^{31}P-MASNMR spectra of α-ZrP evacuated at different temperatures: (A) room temp., (B) 573 K, (C) 773 K, (D) 848 K, (E) 1073 K, (F) 1323 K. * SSB.

nally, α-ZrP evacuated at 1323 K (F in Fig. 7) gives the same spectrum as E in Fig. 6. This result and XRD data (F in Fig. 3) show that the crystals changed to pyro-ZrP. The ^{31}P-MASNMR spectra of ε-ZrP in Fig. 8 showed a different thermal behavior. For evacuation temperatures below 573 K (before condensation of phosphate groups), the spectra gave only one resonance line at −21.7 ppm (A and B in Fig. 8). However, after evacuation at 773 K (after condensation of phosphate groups), the spectra showed a resonance peak with broader linewidth at −37.8 ppm, which was similar to the magnetic field for pyro-ZrP. As was stated previously, this crystal has a very small amount of phosphate groups. In addition, the ^{31}P-MASNMR spectrum of pyro-ZrP(syn) showed a spectrum similar to that of D in Fig. 8. These synthetic zirconium

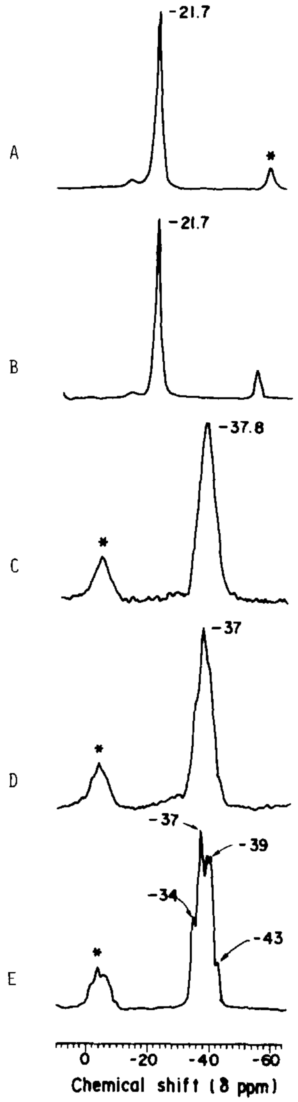

FIG. 8. ^{31}P-MASNMR spectra of ε-ZrP evacuated at different temperatures: (A) room temp., (B) 573 K, (C) 773 K, (D) 873 K, (E) 1473 K. * SSB.

diphosphate crystals prepared at lower temperature and ε-ZrP evacuated at 773 K (C in Fig. 8) showed higher catalytic activities for acid catalyzed reactions.

CONCLUSIONS

The ^{31}P-MASNMR resonance peaks of α-ZrP, ZrP-gel, and ε-ZrP are −16.6, −19.3, and −21.7 ppm, respectively. This order corresponds to fewer and fewer waters of crystallization; thus the layer separation presumably become narrower as well. That is to say when the phosphorus–phosphorus separations above and below Zr atom planes become shorter, the resonance peaks shifted toward higher magetic fields.

We compared the catalytic activities and ^{31}P-MASNMR spectra for ZrP. The ZrP catalysts which show higher catalytic activities for butene isomerization showed the higher magnetic field resonance at around −38 ppm. These active catalysts were ε-ZrP and pyro-ZrP(syn) after evacuation at 773 K. The chemical formulae of those catalysts are almost equivalent to ZrP_2O_7, but they have small amounts of residual phosphate groups on the surface. The ^{31}P-MASNMR results suggest that the residual phosphate groups may enhance the protonic characteristics, since those catalysts showed higher magnetic fields than others. When the accumulation of electrons around phosphorus atoms has occurred, the electrons moved from the residual phosphate groups on the surface to lattice phosphorus atoms; this movement facilitates the acidic properties of catalysts. The IR data for ε-ZrP supported this interpretation: since P–O–P bonds between Zr atom planes were observed after evacuation at higher temperatures (*2*), those P–O–P bonds could withdraw the electrons from the surface.

REFERENCES

1. Alberci, G., and Castantino, U., *in* "Intercalation Chemistry" (M. S. Wittingham and A. J. Jacobson, Eds.), p. 147. Academic Press, New York, 1982.

2. Segawa, K., Kurusu, Y., Nakajima, Y., and Kinoshita, M., *J. Catal.* **94,** 491 (1985).

3. Segawa, K., Kurusu, Y., and Kinosita, M., *in* "Catalysis by Acids and Bases" (B. Imerik, C. Naccache, G. Coudurier, Y. Ben Taarit, and J. C. Vedrine, Eds.), p. 183. Elsevier, Amsterdam, 1985.

4. Clearfield, A., and Stynes, J. A., *J. Inorg. Nucl. Chem.* **26,** 117 (1964).

5. Levi, D. G. R., and Reyronel, G., *Z. Kristallogr.* **92,** 190 (1935).

6. Clearfield, A., and Pack, S. P., *J. Inorg. Nucl. Chem.* **37,** 1283 (1975).

7. Alberti, G., *Acc. Chem. Res.* **11,** 163 (1978).

8. Horsley, S. E., and Nowell, D. V., *J. Appl. Chem. Biotechnol.* **23,** 215 (1973).
9. Troup, J. M., and Clearfield, A., *Inorg. Chem.* **16,** 3311 (1977).
10. Clearfield, A., Blessing, R. H., and Stynes, J. A., *J. Inorg. Nucl. Chem.* **30,** 2249 (1968).
11. Corbridge, D. E. C., *in* "The Structure Chemistry of Phosphorous," p. 130. Elsevier, Amsterdam, 1974.
12. Clearfield, A., Landis, A. L., Media, A. S., and Troup, J. M., *J. Inorg. Nucl. Chem.,* **35,** 1099 (1973).